Optical Quantum Communications: An Experimental Approach

Armando N. Pinto[a,b], Álvaro J. Almeida[a], Nuno A. Silva[a,b], Nelson J. Muga[a,c], and Luís M. Martins[a,c]

[a]Instituto de Telecomunicações, University of Aveiro, 3810-193 Aveiro, Portugal;
[b]Department of Electronics, Telecommunications and Informatics, University of Aveiro, 3810-193 Aveiro, Portugal;
[c]Department of Physics, University of Aveiro, 3810-193 Aveiro, Portugal

ABSTRACT

Quantum laws can be used to implement secure communication channels; this has been named quantum cryptography. In quantum cryptography the security does not depend of limited computational power, but is inherent to the laws that govern the propagation and detection of single and entangled photons. We show how single and entangled photon-pairs can be efficiently generated using four-wave mixing in optical fibers. We analyze the source statistics, degree of entanglement and impact of spontaneous Raman scattering. By coding information in the photons polarization we are able to transmit quantum information over 20 km of standard single mode fiber.

Keywords: Photon Source, Four-Wave Mixing, Polarization, Quantum Communication.

1. INTRODUCTION

The idea of code information in an absolutely secure way has its roots in Stephen Wiesner's work.[1] Following Wiesner's idea, Bennett and Brassard developed the first quantum protocol, the famous BB84,[2] and a few years later, the protocol was successfully tested experimentally.[3]

Although the BB84 protocol uses four quantum states, Bennett found that only two nonorthogonal states of polarization are needed in order to implement quantum cryptography, and then the B92 protocol was developed.[4] Since then, many other protocols were developed and tested for single photons, and entangled photon-pairs.[5]

In order to implement quantum protocols, single-photon or quasi single-photon sources are necessary.[6] A true single-photon source is hard to obtain, but some good approximations have been proposed.[7] The one from an attenuated laser is the more simple and easy to implement.[6]

Recently, we have implemented a single-photon source based on the stimulated four-wave mixing (SFWM) process, that allows us to took advantage of the high nonlinearities present in a dispersion-shifted fiber (DSF).[8–10] The SFWM process is a third-order nonlinear process that is described by the third-order nonlinear susceptibility, $\chi^{(3)}$, originated from the nonlinear response of bound electrons to an applied optical field.[11] This source can be obtained in a low power regime and allows to avoid the losses in the coupling components, since the photons are already generated inside an optical fiber.[10]

We present a review of the work that we have been carrying out in the last few years in the development of quantum communications systems.

Further author information: (Send correspondence to Armando N. Pinto)
Armando N. Pinto: E-mail: anp@ua.pt, Telephone: +351 234377900
Álvaro J. Almeida: E-mail: aalmeida@av.it.pt, Telephone: +351 234377900
Nuno A. Silva: E-mail: nasilva@av.it.pt, Telephone: +351 234377900
Nelson J. Muga: E-mail: muga@av.it.pt, Telephone: +351 234377900
Luís M. Martins: E-mail: lmartins@av.it.pt, Telephone: +351 234377900

This paper is organized in 5 sections. In section 2, we present the single-photon source based on the SFWM process, that we have been used for generate single photons in optical fibers. A brief theoretical description of the process in a low power regime is presented, and the photon statistics of the source reconstructed. Finally, we test the feasibility of the source, using it to encode information into polarization, transmit it through an optical fiber with several kilometers long, and decode it. In section 3, we show the results of the test of one of Bell's inequality, using an entangled photon-pair source from spontaneous four wave mixing (SpFWM). In section 4, we present a real-time polarization compensation scheme based on time-division multiplexing (TDM), and present a model for the quantum bit error rate (QBER). Finally, in section 5 we present the main conclusions of this work.

2. STIMULATED FOUR-WAVE MIXING IN OPTICAL FIBERS

2.1 Single-Photon Source Based on SFWM

The schematics of the experimental setup that we use to implement a single-photon source based on the SFWM process is presented in Fig. 1. This source allows the generation of single photons inside a DSF. These photons are easily coupled to standard single mode fibers for long distance quantum communications.

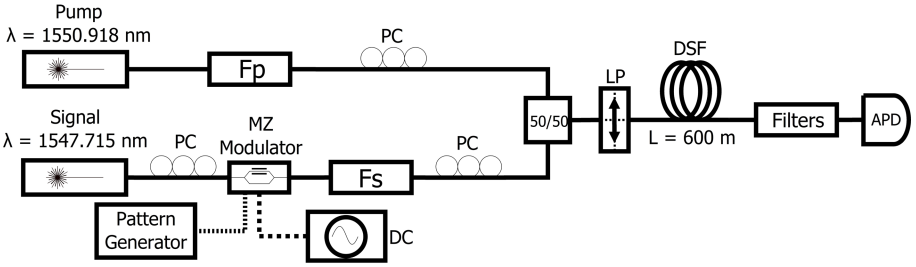

Figure 1. Schematics of the experimental setup used to generate single photons from stimulated four-wave mixing.

A pump from a tunable laser source (TLS), centered at $\lambda_p = 1550.918$ nm, is coupled with an optical signal from and external cavity laser (ECL), centered at $\lambda_s = 1547.715$ nm. The signal wave is modulated with a Mach-Zehnder in order to generate pulses with a full width at half maximum (FWHM) of approximately 1 ns and a repetition rate, $R \approx 1.22$ MHz. Both signals are sent linearly co-polarized to a dispersion-shifted fiber (DSF) with a length equal to 600 m and a nonlinear coefficient, $\gamma \approx 2.3\ \mathrm{W^{-1}km^{-1}}$. Due to the SFWM process, a third wave, known as idler, is generated inside the DSF. Then, pump and signal photons are suppressed by a cascade of optical filters. The detection is performed with InGaAs/InP avalanche photodiodes (APDs), operating in Geiger mode.[12]

2.2 Stimulated Four-Wave Mixing Process in a Low Power Regime

Most of the experiments using the FWM process have been done in a high power regime.[13] However, the FWM process can be obtained in a low power regime.[10]

The nonlinear Schrödinger equation describes the evolution of the electrical field complex amplitudes inside an optical fiber, considering the slowly varying envelope approximation,

$$\frac{\partial A}{\partial z} + \frac{\alpha}{2}A = \sum_{m=2}^{+\infty} \frac{i^{m+1}\beta_m}{m!}\frac{\partial^m A}{\partial t^m} + i\gamma\left[1 + \frac{i}{\omega_0}\frac{\partial}{\partial t}\right]P^{NL}(z,t)\,, \tag{1}$$

where β_m is the dispersion coefficient of m^{th} order, and $P^{NL}(z,t)$ is the third-order nonlinear polarization, given by

$$P^{NL}(z,t) = A(z,t)\int_{-\infty}^{+\infty} R(\tau)|A(z,t-\tau)|^2 d\tau\,, \tag{2}$$

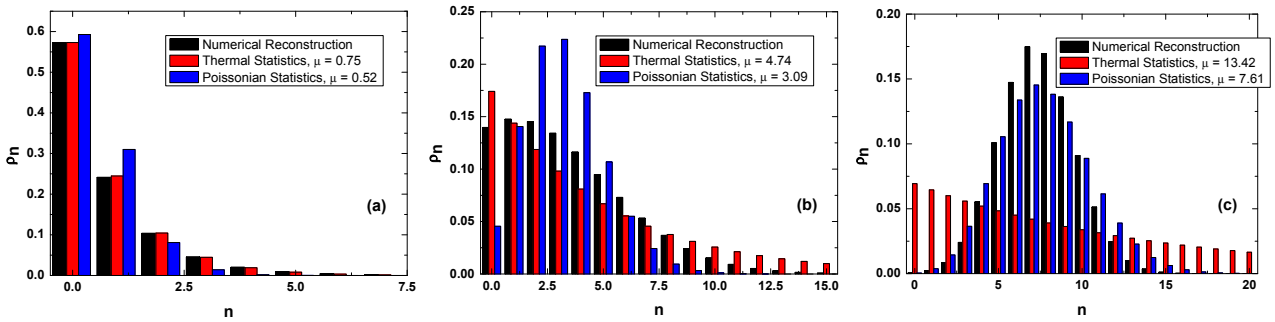

Figure 2. Reconstruction of the photon number distribution for a single-photon source obtained from the SFWM process, and comparison with Thermal and Poissonian statistics.

and $R(\tau)$ is the nonlinear response function of the fiber.[11]

The optical power of the idler wave, P_i, that is generated inside the DSF can be written as

$$P_i(z) = (\gamma P_{\rm p}(0) z_{\rm eff})^2 P_{\rm s}(0) \left| \frac{\sinh(\kappa z)}{kz} \right|^2 \exp\{-\alpha z\}\,, \tag{3}$$

where κ is the parametric gain, and $P_{\rm p}(0)$ and $P_{\rm s}(0)$ are the input pump and signal powers, respectively.[10]

The FWM process will be as much efficient as the pump and signal fields are co-polarized. In case of polarization decorrelation, the FWM process efficiency will decrease, and the nonlinear parameter, γ, will be reduced. A new parameter called effective nonlinear parameter, $\gamma_{\rm eff}$, which is dependent on the pump and signal wavelength separation can be written as[10]

$$\gamma_{\rm eff}(\Delta\lambda) = \frac{8\gamma}{9} + \frac{\gamma}{9}{\rm sech}\left(\frac{(\Delta\lambda)^{A_0}}{T_0} \right), \tag{4}$$

where A_0 and T_0 are fitting parameters, and $\Delta\lambda = \lambda_p - \lambda_s$.

Using SFWM, and adjusting the spectral separation between pump and signal we are able to generate pulses with an adjustable number of photon per pulse in average. In most of our experiments, we work with a very low number of photons, much less than one photon per pulse in average.

2.3 Photon Number Distribution of SFWM Source

In order to characterize the single-photon source based on the SFWM, we have used single photon photodetectors and the maximum-likelihood estimation (MLE) method to reconstruct the photon number statistics.[14] The experimental setup used was the same as presented in Fig. 1, with an extra variable optical attenuator (VOA) between the filters and the APD.

In Fig. 2 we present the numerical reconstruction for three different input powers of the signal, considering that the input pump power is fixed.

We verified that for a low number of photons per pulse, *i.e.* $\mu \leq 1$, the photon number distribution follows a thermal statistics, Fig. 2a), that will change to a Poissonian statistics, Fig. 2c), for a higher number of photons per pulse.

The knowledge of the source statistics provides fundamental information to assess the security of quantum cryptographic transmission systems.

2.4 Polarization-Encoding, Transmission and Detection of Single-Photons

In order to send quantum information, we have used the developed source and we encode information into photons polarization, after we transmit the photons through a standard single-mode fiber with a length equal to 20 km. At the receiver photons are detected and the information is extracted from the photons polarization. The schematics of the experimental setup used in the laboratory, is presented at Fig. 3a). Following the setup presented at Fig. 1, adding a linear polarizer (LP) and a half wave-plate (HWP) at the output of the single-photon source, we can obtain two nonorthogonal linear states of polarization (SOPs). The LPs before the APDs compensate the polarization rotation due to the fiber birefringence. Detectors have a dark count probability per time gate, $t_g = 5$ ns, $P_{dc} < 1.3\times10^{-5}$ ns^{-1}, and the quantum detection efficiency is $\eta_D \approx 10\%$.[12] From the APDs we register the number of clicks in a time interval of 20 s, and the total number of gates that were open in the same time interval. We use an average number of photons per pulse of $\mu \approx 0.2$.

The average number of photon counts registered in each APD can be written as,[15]

$$C = RP_{\text{click}}\,, \tag{5}$$

where R is the pulse repetition rate, and $P_{\text{click}} = P_d + P_{dc} - P_d P_{dc}$, being P_{dc} the probability of having a dark count, and P_d is the probability of detection, that is given by,[16]

$$P_d = \left\{1 - \frac{1}{(1+\frac{\eta_F\eta_B\eta_D\mu}{2})}\right\} \times \left\{\frac{1}{2}\Big(1+\cos(2\theta)\cos(2\phi)\Big) + 2\cos(\theta)\cos(\phi)\sin(\theta)\sin(\phi)\cos(\xi)\right\}. \tag{6}$$

In Fig. 3b) we show the average number of photon counts as a function of the HWP angle, along with the theoretical prediction given by 5. The pump and signal optical powers at the DSF input were $P_p(0) = 2.2$ mW, and $P_s(0) = 2.65\times10^{-3}$ mW, respectively.

From Fig. 3b), we can see that we can encode information into photons polarization, transmit it through a quantum channel with several kilometers long and decode it correctly. As can be seen, the 45° separation between the the nonorthogonal SOPs are maintained.

3. SPONTANEOUS FOUR-WAVE MIXING IN OPTICAL FIBERS

3.1 Entangled-Photon Source Based on SpFWM

The spontaneous four-wave mixing (SpFWM) process can be used to generate entangled photon-pairs in optical fibers. In Fig. 4a), we present the schematics of an experimental setup that we have used to generate entangled

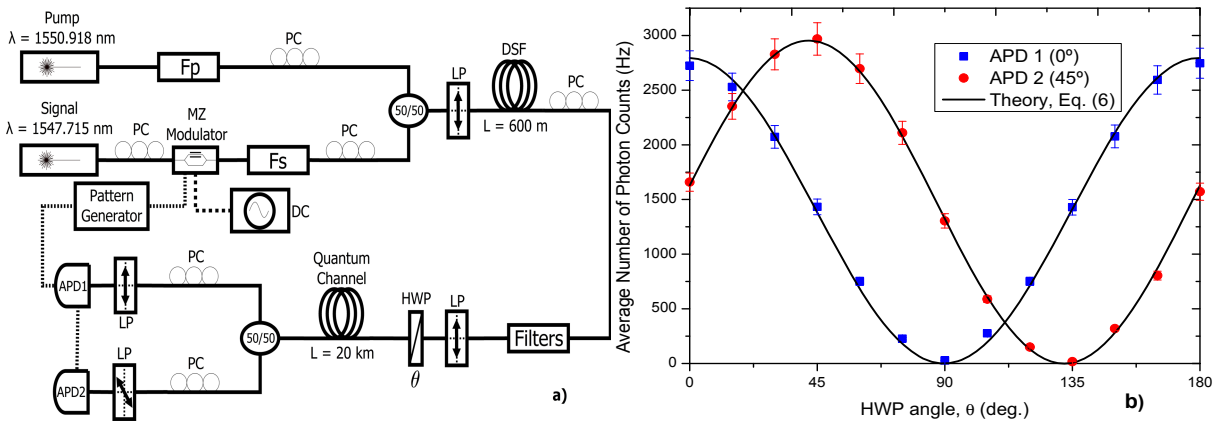

Figure 3. a) Schematics of the experimental setup used to generate, transmit and detect single photons from a single-photon source based on SFWM. b) Average number of photon counts as a function of the HWP angle, for the linear SOPs with angles $\theta = 0°$ and 45°, after propagation through a quantum channel with a length equal to 20 km. The error bars are a 5% deviation for each value.

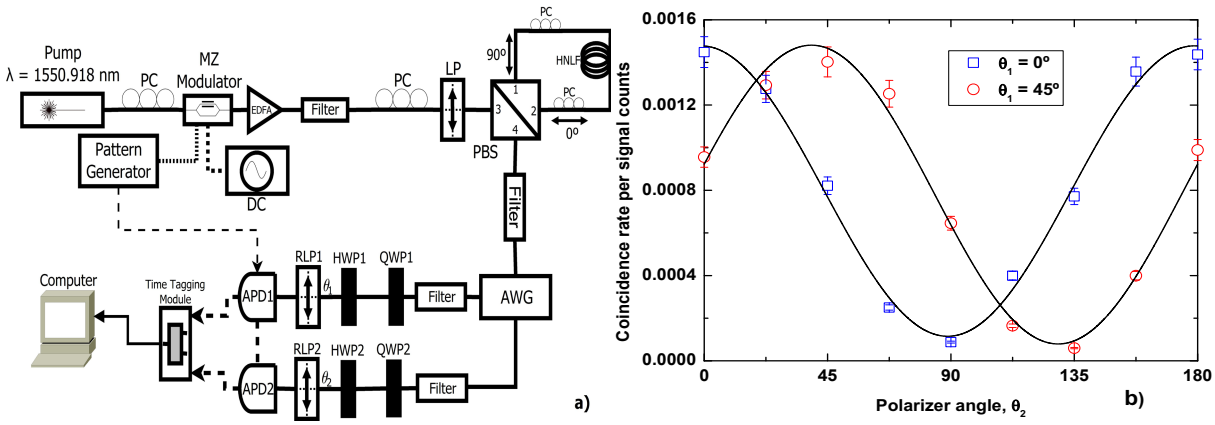

Figure 4. a) Schematics of the experimental setup used to generate polarization-entangled photon-pairs in a Sagnac fiber loop. b) Coincidence rate per signal counts as a function of the linear polarizer angle, θ_2, when θ_1 =0° and 45°. The solid curve is a sinusoidal fit to the experimental data.

photon-pairs encoded into polarization, and to verify the violation of Clauser-Horne-Shimony-Holt (CHSH) inequality.

A pump from a tunable laser source (TLS) is externally modulated with a Mach-Zehnder in order to produce pulses with a full width at half maximum (FWHM) of ≈ 1 ns and a repetition rate, $R \approx$ 2.2 MHz. Next it is sent to an highly nonlinear fiber (HNLF) that is inside of a Sagnac loop. At the output of the loop (port-4 of the polarization beam splitter, PBS), a filter is used to suppress the pump, and the idler and signal waves generated in the loop pass through an arrayed waveguide grating (AWG), which sends signal photons to one path, and idler photons to the other. The states of polarization of the signal and idler photons are adjusted using a quarter waveplate (QWP) and a half waveplate (HWP) so that both photons experience the same polarization change after they were separated by the AWG. Each photon was lead into a rotatable linear polarizer (RLP1 and RLP2) and was detected with an InGaAs/InP avalanche photodiode (APD). The detectors have a dark count probability per time gate, t_g =2.5 ns, of $P_{dc} < 1.3\times10^{-6}$ ns^{-1}, and a quantum detection efficiency, $\eta_D \sim 10\%$.[12] In order to avoid afterpulses, a 10 μs deadtime was applied in both detectors. The electric signals from the APDs were input into a time tagging module (TTM) for coincidence measurements. The TTM worked in a continuous mode, with a time resolution of 82.3 ps.

3.2 Violation of CHSH Inequality

We have implemented the experimental setup presented in Fig. 4a), that allows us to generate polarization-entangled photon-pairs in a Sagnac fiber loop, and measured the coincidence rate for 16 combinations of the polarizer settings (θ_1 = -45°, 0°, 45°, 90°; θ_2 = -22.5°, 22.5°, 67.5°, 112.5°).[17] In order to verify the violation of CHSH inequality, the Shannon parameter, must be $S > 2$.[17]

In Fig. 4b), we present coincident and single counts detected over 60 s, varying the RLP2 (θ_2), while the RLP1 (θ_1) is fixed for values 0°, 45° and 90°, -45°. Results for coincidence counts show that our source produces entangled photon pairs with strong correlation and a visibility greater than 86%. In Fig. 4b) we present signal single counts, as in Fig. 4b) are presented idler single counts, just as an example, since the other results obtained experimentally present similar behavior.

From the measured values we obtained a parameter S = 2.47 ± 0.17, when accidental coincidences were subtracted. Thus, we observed a violation of CHSH inequality by 2.7 standard deviations. Coincidence fringes present visibilities greater than 86%. The fact that the visibility was not much high is due to the spontaneous Raman scattering (SpRS), that contributes for background counts.[18]

4. QKD SYSTEMS WITH POLARIZATION ENCODING

In order to avoid quantum errors and make polarization encoding feasible both TDM- and WDM-based polarization control schemes solutions were proposed in the literature.[19–21] Some control schemes use classical signals

as reference SOPs,[21,22] whereas others schemes use pulses with a low mean number of photons per pulse.[19,20,23] Reference pulses can be sent with[19,20] and without[21–23] interruption of the quantum channel.

4.1 Real-Time Polarization Compensation

A general control scheme for QKD based on TDM is illustrated in Fig. 5. Reference and data signals are time

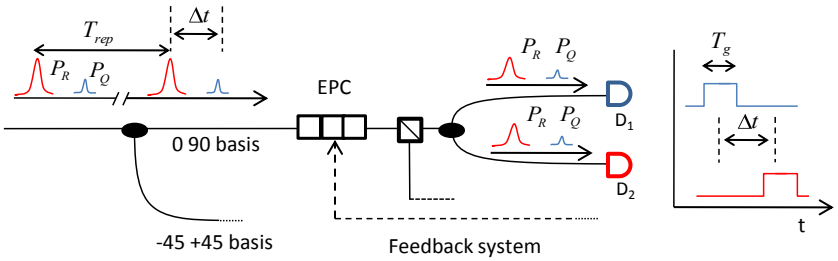

Figure 5. Schematic representation of the TDM-based SOP control scheme. After passing through the PBS the signals are splitted and both signals are present in the data and reference arms. Data and reference gates are delayed by Δt, which corresponds to the data and reference pulses delay.

multiplexed and separated by Δt. A correct synchronization of detector gates assures that data and reference pulses are detected at D_1 and D_2, respectively. The feedback system uses the count records of D_2 to actuate on the electronic polarization controller (EPC) in order to align the input photons with vertical polarization with the vertical port of the PBS.

4.2 QBER for TDM based SOP control schemes

The quantum bit error rate (QBER) is the parameter used to quantify the amount of errors presented in QKD systems. The total QBER is the sum of several different contributions, likewise the intrinsic fiber birefringence, the non ideal polarization isolation of some components, or other sources related with SOP control schemes. The QBER can be defined as the ratio between the wrong detections and total detections. In terms of rates we have,[6] $QBER = N_{\text{wrong}}/(N_{\text{right}} + N_{\text{wrong}}) \approx R_{\text{error}}/R_{\text{shift}}$, where R_{error} represents the rate of error and R_{shift} is the rate of the shifted key,

$$R_{\text{shift}} = 1/2 f_{\text{rep}} \langle n \rangle t_{\text{link}} \eta_{\text{det}}, \tag{7}$$

with f_{rep} being the pulse rate, $\langle n \rangle$ the mean number of photons per pulse, η_{det} the detector efficiency, and $t_{\text{link}} = 10^{-\alpha z/10}$ the transmission efficiency (α and z are the fiber losses and length, respectively).

For SOP control systems with reference signals multiplexed in the time domain, the main contributions to the total QBER are the time decorrelation between reference and data SOPs ($QBER_{\text{tACF}}$), the feedback SOP control system limitations ($QBER_{\text{SOP}}$), the leakage of photons from the reference pulse to the data gate ($QBER_{\text{leak}}$), the detector afterpulse probability ($QBER_{\text{af}}$), and the dark counts ($QBER_{\text{dc}}$). The expression for the total $QBER$ can be written as[24]

$$\begin{aligned} QBER =& QBER_{\text{tACF}} + QBER_{\text{SOP}} + QBER_{\text{leak}} + QBER_{\text{af}} + QBER_{\text{dc}} = \\ =& 1/4 - 1/4 \exp(-3\omega^2 D_{\text{p}}^2 z \left|T_{\text{rep}} - \Delta t\right| / (2t_0)) + 1 - \cos^2(1/2\,\Theta(1 - \exp(-g T_{\text{rep}}))) + \\ &+ \frac{1}{2}\frac{\langle n_{\text{r}} \rangle A}{\langle n \rangle} + \frac{\langle n_{\text{r}} \rangle P_{\text{af}}}{\langle n \rangle \eta_{\text{det}}} + \frac{1}{2}\frac{P_{\text{dc}} n_{\text{det}}}{\langle n \rangle t_{\text{link}} \eta_{\text{det}}}, \end{aligned} \tag{8}$$

where T_{rep} is the inverse of the pulse rate (f_{rep}), Δt is the temporal separation between the reference and data pulses, t_0 represents the drift time of the index difference between the fast and slow fiber axes, Θ and g are parameters related with the feedback SOP control,[24] η_{det} is the quantum detector efficiency, P_{af} is the afterpulse probability, $\langle n_{\text{g}} \rangle = A \langle n_{\text{r}} \rangle$ is the mean number of reference photons per pulse leaked to the data detector gate, with $\langle n_{\text{r}} \rangle$ being the mean number of reference photons per pulse, and the parameter A the fraction of photons that are leakage to the wrong detector.

Figure 6 shows the different contributions the total QBER (given by (8)), as a function of propagation distance, z. The following parameters values were used in order to plot the map: $\beta_2 = -20$ ps^2/km, $\langle n_r \rangle = 4$,

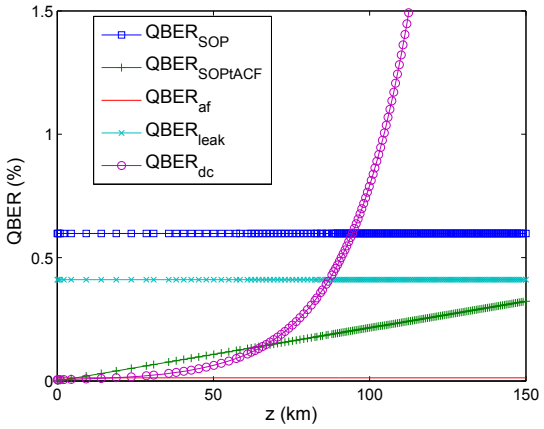

Figure 6. Representation of the different QBER contribution as a function of the distance.

$\langle n \rangle = 0.1$, $\alpha = 0.22$ dB/km, $T_{\mathrm{FWHM}} = 1$ ns, $\Delta t = 100$ ns, $D_p = 0.2$ ps/km$^{1/2}$, $T_g = 2$ ns, $\eta_{\mathrm{det}} = 10\%$, $g_{\mathrm{af}} = 2.77\times10^{-12}$ s, $t_0 = 8.5\times10^{7}$ s, $P_{\mathrm{dc}} = 1\times10^{-6}$, $\Theta = \pi/2$ rad, and $g = 0.5 \times10^{2}$ s^{-1}.

The fiber losses become dominant for distances longer than 100 km.

5. CONCLUSIONS

We presented our recent work on quantum communications. We present our single-photon source based on SFWM, as discuss the source statistcs. We show how information can be encoded and decoded from photons polarizations. We also show how the scrambling of polarization that occurs due to propagation in a birefringent medium, as an optical fiber, can be compensated. Using the spontaneous four-wave mixing process, we developed an entangled-photon source and verified the violation of Clauser-Horne-Shimony-Holt inequality. We also developed a model for quantum bit error rate estimation.

ACKNOWLEDGMENTS

This work was partially supported by the Fundação para a Ciência e Tecnologia, FCT, through the Laboratório Associado (IT/LA) program, project "QuantTel - Quantum Secure Telecommunications" and "QuantPrivTel - Quantum Private Telecommunications" project (PTDC/EEA-TEL/103402/2008), FEDER and PTDC programs.

REFERENCES

[1] Wiesner, S., "Conjugate coding," *SIGACT News* **15**(1), 78–88 (1983).

[2] Bennett, C. H. and Brassad, G., "Quantum cryptography: Public-key distribution and coin tossing," *Proceedings of IEEE International Conference on Computers, Systems and Signal Processing, Bangalore, India* , 175 – 179 (Dec. 1984).

[3] Bennett, C. H. and Brassad, G., "The dawn of a new era for quantum cryptography: The experimental prototype is working!," *Sigact News* **20**(4) (1989).

[4] Bennett, C. H., "Quantum cryptography using any two nonorthogonal states," *Physical Review Letters* **68**, 3121–3124 (May 1992).

[5] Ekert, A. K., "Quantum cryptography based on Bell's theorem," *Physical Review Letters* **67**, 661–663 (Aug. 1991).

[6] Gisin, N., Ribordy, G., Tittel, W., and Zbinden, H., "Quantum cryptography," *Reviews of Modern Physics* **74**, 145–195 (Jan. 2002).

[7] Lounis, B. and Orrit, M., "Single-photon sources," *Reports on Progress in Physics* **68**, 1129–1179 (May 2005).

[8] Antunes, P. F., Pinto, A. N., and André, P. S., "Single-photon source by means of four-wave mixing inside a dispersion-shifted optical fiber," in [*Frontiers in Optics*], FMJ3, Optical Society of America (Oct. 8-12, 2006).

[9] Almeida, A. J., Fernandes, G. G., and Pinto, A. N., "Single-Photon Source With Adjustable Linear SOP," in [*Proceedings of the VII Symposium On Enabling Optical Networks and Sensors*], (June 26, 2009).

[10] Silva, N., Muga, N., and Pinto, A., "Effective nonlinear parameter measurement using fwm in optical fibers in a low power regime," *Quantum Electronics, IEEE Journal of* **46**(3), 285 –291 (2010).

[11] Agrawal, G., "Nonlinear Fiber Optics, 4th ed.," *Academic Press* (2007).

[12] Ribordy, G., Gisin, N., Guinnard, O., Stucki, D., Wegmuller, M., and Zbinden, H., "Photon counting at telecom wavelengths with commercial InGaAs/InP avalanche photodiodes: current performance," *Journal of Modern Optics* **51**, 1381–1398 (Sept. 2004).

[13] Inoue, K., "Four-wave mixing in an optical fiber in the zero-dispersion wavelength region," *Journal of Lightwave Technology* **10**, 1553–+ (1992).

[14] Rossi, A. R., Olivares, S., and Paris, M. G. A., "Photon statistics without counting photons," *Phys. Rev. A* **70**, 055801 (Nov 2004).

[15] Trifonov, A., Subacius, D., Berzanskis, A., and Zavriyev, A., "Single photon counting at telecom wavelength and quantum key distribution," *Journal of Modern Optics* **51**, 1399–1415 (Sept. 2004).

[16] Almeida, A. J., Silva, N. A., Muga, N. J., and Pinto, A. N., "Single-photon source using stimulated fwm in optical fiber for quantum communication," in [*International Conference on Applications of Optics and Photonics, AOP'2011*], SPIE (May 3-7, 2011).

[17] Clauser, J. F., Horne, M. A., Shimony, A., and Holt, R. A., "Proposed Experiment to Test Local Hidden-Variable Theories," *Physical Review Letters* **23**, 880–884 (Oct. 1969).

[18] Almeida, l. J., Carneiro, S. R., Silva, N. A., Muga, N. J., and Pinto, A. N., "Time coincidence of entangled photon pairs using spontaneous four-wave mixing in a fiber loop," *VIII Symposium On Enabling Optical Networks and Sensors, INESC, Porto, Portugal* (June 25 2010).

[19] Chen, J., Wu, G., Li, Y., Wu, E., and Zeng, H., "Active polarization stabilization in optical fibers suitable for quantum key distribution," *Opt. Express* **15**(26), 17928–17936 (2007).

[20] Cheng-Zhi, P., Jun, Z., Dong, Y., Wei-Bo, G., Huai-Xin, M., Yin, H., Zeng, H.-P., Tao, Y., Xiang-Bin, W., and Jian-Wei, P., "Experimental long-distance decoy-state quantum key distribution based on polarization encoding," *Phys. Rev. Lett.* **98**, 010505 (Jan 2007).

[21] Xavier, G. B., de Faria, G. V., ao, G. P. T., and von der Weid, J. P., "Full polarization control for fiber optical quantum communication systems using polarization encoding," *Opt. Express* **16**(3), 1867–1873 (2008).

[22] Xavier, G. B., Walenta, N., de Faria, G. V., Temporo, G. P., Gisin, N., Zbinden, H., and von der Weid, J. P., "Experimental polarization encoded quantum key distribution over optical fibres with real-time continuous birefringence compensation," *New J. Phys.* **11**(4), 045015 (2009).

[23] Chen, J., Wu, G., Xu, L., Gu, X., Wu, E., and Zeng, H., "Stable quantum key distribution with active polarization control based on time-division multiplexing," *New J. Phys.* **11**(6), 17928–17936 (2009).

[24] Muga, N. J., Mário F. S. Ferreira, and Pinto, A. N., "QBER estimation in QKD systems with polarization encoding," *IEEE/OSA J. Lightwave Technol.* **29**(3), 355 – 361 (2011).